

# Denoising Algorithm for Medical Ultrasound Image Based on 2D-VDM and PM

Manyu Yan

School of Communication Engineering  
Chengdu University of Information Technology  
Chengdu, China

Chengyu Wen

School of Communication Engineering  
Chengdu University of Information Technology  
Chengdu, China

---

**Abstract:** In order to solve the problem of several common methods in medical ultrasound image processing which includes Poor retention of detailed information and insignificant denoising effect, therefore a new method of ultrasonic image denoising combining two-dimensional variational mode decomposition (abbreviated as 2D-VDM) and anisotropic diffusion (abbreviated as PM) is proposed. This method firstly decomposes the image into a series of modal component (IMF) images through two-dimensional variational mode decomposition (2D-VDM), and then uses the peak signal-to-noise ratio and the normalized mean square error to filter out the effective modal components, finally, the effective modal components are subjected to anisotropic diffusion (PM) filter processing and reconstruct the processed effective components to remove image noise. The evaluation of image quality indicators from peak signal-to-noise ratio and root mean square error shows that this method is superior to other commonly used methods in removing noise and protecting detailed information in the image.

**Keywords:** Ultrasound image; two-dimensional variational modal decomposition; anisotropic diffusion; modal component

---

## 1. INTRODUCTION

At present, ultrasound imaging equipment is becoming more and more popular, such as portable remote medical ultrasound scanning instruments. In the ultrasound imaging process, speckle noise will be formed due to the strength and difference of the signal, which causes the image will be unclear. Therefore, the image denoising technology plays a vital role, which can obtain higher quality and clearer images from the ultrasound equipment, so that the tissues inside the human body can be observed more clearly [1]. The current image denoising methods are generally divided into two categories: time domain and frequency domain denoising methods. The denoising process in the time domain mainly uses the corresponding processing function to convolve with the image containing noise to process the pixels in the image. The denoising process in frequency domain mainly decomposes the image into multiple frequencies in different ranges to obtain the corresponding frequency characteristics. Time domain denoising methods include linear filtering methods (first-order statistical filtering, higher-order statistical filtering), non-linear filtering methods (median filtering, geometric filtering, uniform geometric filtering, etc.). Although these methods have a good effect of removing noise, there is a phenomenon that the edges are over-smoothed, causing loss of detailed information [2]. In order to solve the problem that the edges and details of images are easily blurred, researchers have applied partial differential equations to image processing. Therefore Perona and Malik proposed to use the P-M diffusion equation (PM model) as a filtering method for ultrasound images. The algorithm mainly uses a diffusion function to achieve different diffusion strengths in different directions [3]. The denoising methods in the frequency domain mainly include wavelet transform, curved wave transform, etc. These methods have the same problem that the effect of removing noise depends largely on the choice of the fundamental wave. Therefore, American NASA scientist Huang NE proposed the Empirical Mode Decomposition (EMD) algorithm in 1998, which mainly

decomposes one-dimensional signals into different intrinsic modal components (IMF) [4]. In 2001, Song Pingjian and others extended the empirical mode decomposition method to the two-dimensional range, that is the two-dimensional empirical mode decomposition (BEMD), because the empirical mode decomposition (EMD) algorithm is prone to aliasing and other problems [5]. In 2014, for the problems of this algorithm, research scholars proposed an improved variational mode decomposition algorithm (VMD) based on empirical mode decomposition (EMD). The algorithm mainly seeks the optimal value of each natural modal component (frequency, bandwidth) by variational method, so as to overcome the shortcomings of empirical mode decomposition (EMD) [6]. In addition, VMD has also been extended to a two-dimensional range, that is, two-dimensional variational mode decomposition (2D-VMD).

Two-dimensional variational mode decomposition can decompose the image into low-frequency components and high-frequency components. In addition, anisotropic diffusion filtering is better than other filtering methods in dealing with ultrasonic images in terms of denoising effect and retaining detailed information. This article mainly combines the characteristics of the two methods, and proposes a new method of ultrasonic image denoising that combines two-dimensional variational mode decomposition and anisotropic diffusion. Firstly, the image is decomposed into low-frequency components and high-frequency components through two-dimensional variational mode decomposition, and then anisotropic diffusion filtering is used to filter the low-frequency components, and finally the filtered components are reconstructed.

## 2. TWO-DIMENSIONAL VARIATIONAL MODE DECOMPOSITION (2D-VMD)

Variational modal decomposition decomposes the signal into a series of IMF components, and iterates to determine the IMF

through the entire decomposition process. Firstly, setting the number of modal components (IMF) to be decomposed in advance and performing Hilbert transform on each model function  $u_k(t)$  to obtain its analytical function, and then add an exponential term  $e^{-j\omega t}$  to adjust its center frequency. Secondly, in order to make the decomposed IMF frequency band as close as possible to the center frequency, thus establish a constraint minimization model. Finally, a quadratic penalty term and a Lagrangian multiplier are added to this model to transform its model into an unconstrained model, in addition, iterate its model continuously to find the optimal solution to determine each modal component (IMF).

## 2.1 Two-dimensional analytical signal

Two-dimensional variational mode decomposition is extended in one-dimensional range. In the one-dimensional variational mode decomposition, the Hilbert transform is mainly performed on each mode, which is used as the imaginary part to obtain its one-dimensional analytical signal  $u_k^A(t)$  [7] as in Eq.1.

$$u_k^A(t) = u_k(t) + jH(u_k(t)) = (\sigma(t) + \frac{j}{\pi}) * u_k(t) \quad (1)$$

Fourier transform Eq.1 to obtain one-dimensional analytical signal in frequency domain as in Eq.2.

$$u_k^A(\omega) = (1 + \text{sgn}(\omega)) \cdot u_k(\omega) = \begin{cases} 2u_k(\omega) & \omega > 0 \\ u_k(\omega) & \omega = 0 \\ 0 & \omega < 0 \end{cases} \quad (2)$$

From the above Eq.2. In the one-dimensional domain, the spectrum of the analytic signal has a unilateral characteristic. The existence of this characteristic can adjust the modal spectrum to the corresponding estimated center frequency. For the analytical signal has this characteristic in the two-dimensional range, thus an interface is selected as the center, and a half plane of the interface must be set to 0, where the interface is equivalent to a vector  $w_k$ . Two-dimensional analytical signal  $u_k^{AS}(x)$  as in Eq.3.

$$u_k^{AS}(x) = u_k(x) * (\sigma(\langle x, w_k \rangle) + \frac{j}{\pi} \cdot \langle x, w_k \rangle) \cdot \sigma(w) \quad (3)$$

Fourier transform Eq.3 to obtain a two-dimensional analytical signal in the frequency domain  $u_k^{AS}(\omega)$  as in Eq.4.

$$u_k^{AS}(\omega) = (1 + \text{sgn}(\langle \omega, w_k \rangle)) \cdot u_k(\omega) = \begin{cases} 2u_k(\omega) & \langle \omega, w_k \rangle > 0 \\ u_k(\omega) & \langle \omega, w_k \rangle = 0 \\ 0 & \langle \omega, w_k \rangle < 0 \end{cases} \quad (4)$$

## 2.2 2D-VMD function and solving $u_k$ and $w_k$

### 2.2.1 2D-VMD function

The one-dimensional variational mode decomposition properties are used to define the two-dimensional VMD function. Firstly, the two-dimensional analytical signal of each mode is multiplied by the complex exponential term, then, the bandwidth of each mode is calculated as the gradient mode. Specific formula as in Eq.5.

$$\sum_k \left\| \nabla [u_k^{AS}(x) e^{-j\langle w_k, x \rangle}] \right\|_2^2 \quad (5)$$

The purpose of variational mode decomposition is to make the frequency bandwidth of each mode decomposed as close as possible to its center frequency. Therefore, the above formula is converted into a constrained minimum model as an objective function to evaluate the modal bandwidth, which is two-dimensional VMD function as in Eq.6.

$$\min_{\{u_k\}, \{w_k\}} \left\{ \sum_k \left\| \nabla [u_k^{AS}(x) e^{-j\langle w_k, x \rangle}] \right\|_2^2 \right\} \quad (6)$$

$$s.t. \quad \forall x : \sum_k u_k(x) = f(x)$$

In Eq.6:  $\{u_k\} = \{u_1, u_2, u_3, \dots, u_k\}$ ,  $\{w_k\} = \{w_1, w_2, w_3, \dots, w_k\}$

In order to solve the problem of transforming constrained into unconstrained models, thus using an operator which is multiplication operator alternating direction method (ADMM). The quadratic penalty term has good convergence in the case of finite weight coefficients, and Lagrange multipliers can achieve good constraints [8]. The unconstrained two-dimensional VMD function is obtained as in Eq.7.

$$L(\{u_k\}, \{w_k\}, \lambda) = \sum_k \alpha_k \left\| \nabla [u_k^{AS}(x) e^{-j\langle w_k, x \rangle}] \right\|_2^2 + \left\| f(x) - \sum_k u_k(x) \right\|_2^2 + \langle \lambda(x), f(x) - \sum_k u_k(x) \rangle \quad (7)$$

The ADMM is used to convert the constrained model into an unconstrained model, therefore, the solution of the constrained model is converted into a saddle point for solving the unconstrained model, which is the maximum or minimum value in a certain direction.

### 2.2.2 Solving and Update $u_k$ and $w_k$

#### 2.2.2.1 Update $u_k$

For the problem of solving and updating, which is converted to find the minimum value of the function of Eq.7. The expression is as in Eq.8.

$$u_k^{n+1} = \arg \min_{w_k, u_k \in R} \left\{ \alpha_k \left\| \nabla [u_k^{AS}(x) e^{-j\langle w_k, x \rangle}] \right\|_2^2 + \left\| f(x) - \sum_i u_i(x) + \frac{\lambda(x)}{2} \right\|_2^2 \right\} \quad (8)$$

In Eq.8:  $w_k$  is equal to  $w_k^{n+1}$ ,  $\sum_i u_i(x)$  is equal to  $\sum_{i \neq k} u_i^{n+1}(x)$ .

According to the convolution properties and Fourier transform, the above Eq.8 is further transformed into the frequency domain as in Eq.9.

$$\hat{u}_k^{n+1} = \arg \min_{\hat{u}_k, w_k \in \mathbb{R}} \left\{ \left\| jw[(1 + \text{sgn}(w + w_k))\hat{u}_k(w + w_k)] \right\|_2^2 + \left\| \hat{f}(w) - \sum_1^k \hat{u}_i(w) + \frac{\lambda(w)}{2} \right\|_2^2 \right\} \quad (9)$$

In Eq.9:  $\forall w \in \Omega_k$ ,  $\Omega_k = \{w | \langle w, w_k \rangle > 0\}$  and adjust the first item to  $w \rightarrow w - w_k$ , the above Eq.9 is transformed into the following formula as in Eq.10.

$$\hat{u}_k^{n+1} = \arg \min_{\hat{u}_k, w_k \in \mathbb{R}} \left\{ \left\| j(w - w_k)[(1 + \text{sgn}(w))\hat{u}_k(w)] \right\|_2^2 + \left\| \hat{f}(w) - \sum_1^k \hat{u}_i(w) + \frac{\lambda(w)}{2} \right\|_2^2 \right\} \quad (10)$$

To distribute the bandwidth of the analytical signal of the real signal in the positive half plane  $w \in \{w, w_k\} > 0\}$ . According to Eq.4, adjust the above Eq.10 to the following Eq.11.

$$\hat{u}_k^{n+1} = \arg \min_{\hat{u}_k, w_k \in \mathbb{R}} \left\{ \int_0^{+\infty} 4\alpha_k (w - w_k)^2 |\hat{u}_k(w)|^2 + 2 \left| \hat{f}(w) - \sum_1^k \hat{u}_i(w) + \frac{\lambda(w)}{2} \right|^2 dw \right\} \quad (11)$$

The meaning of the mathematical form of the above Eq.11 is to find the saddle point  $\hat{u}_k$  where the integral in Eq.11 reaches the minimum value in the positive half plane,  $\hat{u}_k$  is the result of the (n + 1)th update. The integral term in the above Eq.11 is denoted as P. To make P the minimum value, find the partial derivative of  $\hat{u}_k$  in the formula P. When the partial derivative is equal to 0, the value of  $\hat{u}_k$  is the result. as in Eq.12.

$$\frac{\partial P}{\partial \hat{u}_k(w)} = 8\alpha_k (w - w_k)^2 \hat{u}_k(w) - 4 \left| \hat{f}(w) - \sum_1^k \hat{u}_i(w) + \frac{\lambda(w)}{2} \right| = 0 \quad (12)$$

According to Eq.12, the result of  $\hat{u}_k(w)$  is  $\hat{u}_k^{n+1}(w)$ , as in Eq.13.

$$\hat{u}_k^{n+1}(w) = \frac{\hat{f}(w) - \sum_{i \neq k} \hat{u}_i(w) + \frac{\lambda(w)}{2}}{1 + 2\alpha_k (w - w_k)^2} \quad (13)$$

The real part after inverse Fourier transform of Eq.13 is the corresponding IMF component  $u_k$ .

### 2.2.2.2 Update $w_k$

Regarding how to update and solve  $w_k$ , make the main center frequency appear in the bandwidth. the objective function is as in Eq.14.

$$w_k^{n+1} = \arg \min_{w_k, u_k \in \mathbb{R}} \left\{ \alpha_k \left\| \nabla [u_k^{AS}(x) e^{-j\langle w_k, x \rangle}] \right\|_2^2 \right\} \quad (14)$$

According to the convolution and Fourier transform and Eq.8, to make the frequency band of each IMF as close as possible to the center frequency, the above Eq.14 is transformed into the frequency domain and the expression is as in Eq.15.

$$w_k^{n+1} = \arg \min_{w_k} \left\{ \int_{\Omega} (w - w_k)^2 |\hat{u}_k(w)|^2 dw \right\} \quad (15)$$

Let the partial derivative of the integral part of Eq.15 for  $w_k$  equal to zero, get the value of  $w_k$  as the result of its (n + 1)th update. as in Eq.16

$$\frac{\partial \left\{ \int_{\Omega} (w - w_k)^2 |\hat{u}_k(w)|^2 dw \right\}}{\partial w_k} = - \int_{\Omega} 2(w - w_k) |\hat{u}_k(w)|^2 dw = 0 \quad (16)$$

According to Eq.16,  $w_k^{n+1}$  can be obtained as in Eq.17.

$$w_k^{n+1} = \frac{\int_{\Omega} w |\hat{u}_k(w)|^2 dw}{\int_{\Omega} |\hat{u}_k(w)|^2 dw} \quad (17)$$

## 2.3 The specific process of 2D-VMD algorithm

Step 1: Initialized the values of  $\{\hat{u}_k^0\}, \{\hat{w}_k^0\}, \hat{\lambda}_k^0, n, k$ .

Step2: According to Eq.13, update  $u_k$  within a certain range.

Step3: According to Eq.17, update  $w_k$  within a certain range.

Step4: Update  $\lambda$ , which is  $\hat{\lambda}^{n+1}(w) = \hat{\lambda}^n(w) + \tau(\hat{f}(w) - \sum_k \hat{u}_k^{n+1}(w))$ .

Step 5: Repeat the above steps continuously, until the number of cycles is greater than n and

$$\sum_k \frac{\|\hat{u}_k^{n+1} - \hat{u}_k^n\|_2^2}{\|\hat{u}_k^n\|_2^2} < \kappa e, \text{ then stop iterating.}$$

## 3. ANISOTROPIC DIFFUSION ALGORITHM (PM ALGORITHM)

In this paper, the PM model (Perona-Malik model) is used to remove the noise of the effective component IMF image decomposed by the 2D-VDM algorithm. The model mainly proposes to replace the diffusion coefficient d with the functional diffusion coefficient on the classical anisotropic diffusion equation[9]. The PM model is as in Eq.18.

$$\begin{cases} \frac{\partial g_{i,j,t}}{\partial t} = \text{div}[f(|\nabla g_{i,j,t}|) \nabla g_{i,j,t}] \\ \frac{\partial g_{i,j,t}}{\partial t} = \left[ \frac{\partial f(|\nabla g_{i,j,t}|)}{\partial i} \frac{\partial g_{i,j,t}}{\partial i} \right] + \left[ \frac{\partial f(|\nabla g_{i,j,t}|)}{\partial j} \frac{\partial g_{i,j,t}}{\partial j} \right] \\ g(i, j, 0) = g_0(i, j) \end{cases} \quad (18)$$

In Eq.18,  $f(|\nabla g_{i,j,t}|)$  is diffusion coefficient function,  $\nabla$  is gradient,  $div$  is divergence,  $g_0(i,j)$  is a starting pixel,  $(i,j)$  is pixel position in the image,  $t$  is Time interval. In the PM model, Perona and Malik proposed two functions that meet the following conditions as in Eq.19,Eq.20.

$$f_1(|\nabla g_{i,j,t}|) = \exp(-|\nabla g_{i,j,t}|/k)^2 \quad (19)$$

$$f_2(|\nabla g_{i,j,t}|) = \frac{1}{1 + (|\nabla g_{i,j,t}|/k)^2} \quad (20)$$

The above medium diffusion coefficient function  $f(|\nabla g_{i,j,t}|)$  should have the following characteristics:

- (1)The function  $f(|\nabla g_{i,j,t}|)$  takes  $|\nabla g_{i,j,t}|$  as a variable and decreases as the variable rises.
- (2)when  $|\nabla g_{i,j,t}| \rightarrow 0, f(|\nabla g_{i,j,t}|) = 1$  .
- (3)When  $|\nabla g_{i,j,t}| \rightarrow 1, f(|\nabla g_{i,j,t}|) = 0$  .

In Eq.19,Eq.20,Constant  $k$  is the gradient threshold.Judging the size relationship between  $k$  and  $|\nabla g_{i,j,t}|$  is mainly used to diffuse a certain range in the image.Discrete Eq.18 as in Eq.21.

$$\frac{\partial g_{i,j,t}}{\partial t} = \lambda \{d_{i+1,j,t} \nabla_N g_{i,j} + d_{i-1,j,t} \nabla_S g_{i,j} + d_{i,j+1,t} \nabla_W g_{i,j} + d_{i,j-1,t} \nabla_E g_{i,j}\} \quad (21)$$

In Eq.21,  $d_{i+1,j,t}, d_{i-1,j,t}, d_{i,j+1,t}, d_{i,j-1,t}$  are the diffusion coefficient values of north, south, east and west respectively and  $\nabla_N g_{i,j}, \nabla_S g_{i,j}, \nabla_W g_{i,j}, \nabla_E g_{i,j}$  represent the upward gradient of north, south, east and west respectively,  $\lambda$  is a measure of the rate of diffusion[10].Then the new pixel value  $f_{i,j}$  after processing is as in Eq.22.

$$f_{i,j} = g_{i,j} + \frac{\partial g_{i,j,t}}{\partial t} \quad (22)$$

In summary, the PM diffusion model can be obtained as in Fig.1

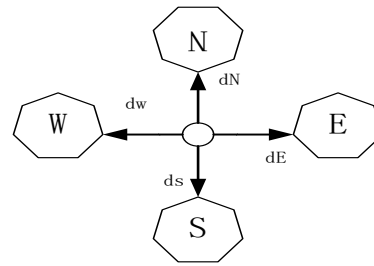


Figure 1. PM diffusion model

#### 4. SPECIFIC STEPS OF MEDICAL IMAGE DENOISING ALGORITHM BASED ON 2D-VDM AND PM

To remove noise and retain the original image features and details to the greatest extent, therefore,this paper proposes an ultrasonic image denoising algorithm based on a combination of two-dimensional variational mode decomposition (2D-VMD) and anisotropic diffusion algorithm (PM).This method firstly decomposes the image into a series of modal component (IMF) images through two-dimensional variational mode decomposition (2D-VDM),and then uses the peak signal-to-noise ratio and the normalized mean square error to filter out the effective modal components, finally, the effective modal components are subjected to anisotropic diffusion (PM) filter processing and reconstruct the processed effective components to remove image noise.Specific steps are as follows:

Step 1:Firstly read the Gaussian speckle noise image and grayscale it to  $g(x,y)$ , and then initialize the values of  $\{\hat{u}_k^0\}, \{\hat{w}_k^0\}, \hat{\lambda}_k^0, n, k$  respectively.

Step 2:Through the 2D-VDM algorithm, the processed grayscale image  $g(x,y)$  is decomposed into k modal component IMF images  $img_k(x,y)$  .

Step3:By evaluating the index coefficients, the k-model component IMF images  $img_k(x,y)$  after decomposition are screened to select effective model image I components.

Step 4: The effective IMF image components are subjected to anisotropic diffusion (PM) processing to obtain the effective modal components after denoising.

Step 5: Reconstruct the filtered effective IMF component image, and the reconstructed image is the denoised image  $\hat{g}(x,y)$  .

## 5. EXPERIMENTAL EVALUATION METHOD AND RESULT ANALYSIS

### 5.1 Experimental evaluation method

For evaluating the effectiveness and performance of the filtering algorithm, it is mainly measured by the two aspects of denoising and protection of detailed information. Therefore, the peak signal-to-noise ratio (PSNR) and root-mean-square error (RMSE) are used to determine the ability to remove noise and retain detailed information respectively[11].

(1) peak signal-to-noise ratio (PSNR)

The peak signal-to-noise ratio is the main evaluation index to measure the filtering algorithm's ability to remove image noise. This indicator counts the changes in the image signal-to-noise ratio, so the value of this indicator (PSNR) is the larger, the filtering algorithm's ability to remove noise is the stronger [12]. Its definition is as in Eq.23.

$$PSNR = 10 \log \frac{M_{\max}(i, j) \times M \times N}{\sum_{i=1}^M \sum_{j=1}^N [g(i, j) - f(i, j)]^2} \quad (23)$$

In Eq.23,  $M_{\max}(i, j)$  is The maximum pixel value of the image after grayscale,  $M, N$  are rows and columns respectively,  $g(i, j)$  is the pixel value of the image after noise removal,  $f(i, j)$  is the pixel value of the initial image,  $M \times N$  is the sum of image pixels.

(2) root-mean-square error (RMSE)

Decide the quality of the image filtering algorithm, an aspect of detail information that needs to be considered. therefore, the root mean square error (RMSE) is selected as the main index for evaluating the image quality. This index mainly describes the similarity of the original image and the denoised image in pixels. If the value is smaller, the higher the degree of similarity is the higher and the ability to maintain details is the stronger[13]. Its definition is as in Eq.24.

$$RMSE = \sqrt{\frac{1}{M \times N} \sum_{i=1}^M \sum_{j=1}^N [g(i, j) - f(i, j)]^2} \quad (24)$$

In Eq.24,  $g(i, j)$  is the pixel value of the image after noise removal,  $M \times N$  is the sum of image pixels,  $f(i, j)$  is the pixel value of the initial image.

### 5.2 Result analysis

To verify whether the method in this paper can better remove noise while retaining detailed information, three

groups of experiments are mainly carried out, which selects two groups of ultrasound fetal and ultrasound kidney images by Field tool simulation and a set of standard images [14]. In the actual ultrasonic reflected wave imaging process, it will be interfered by various waves, which results in speckle noise on the ultrasound image with different brightness levels. In addition, the noise is random and its phase distribution and probability density function obey Gaussian distribution. Due to the uncertainty of noise in the ultrasound imaging process, the Gaussian noise variances of 0.02 and 0.05 were added to the three groups of images, respectively, in order to verify the effectiveness of the proposed algorithm in removing the different noise intensity. In addition, Wiener filtering, median filtering, PM filtering, 2D-VDM combined with median filtering and the method in this paper are applied to ultrasound images, finally, the denoising performance of various methods is evaluated by comparing the two coefficients of peak signal-to-noise ratio and root mean square error.

For better filtering processing later, the peak signal-to-noise ratio and the root mean square error are used as evaluation indicators to filter out the effective IMF image components in the ultrasound image after two-dimensional variational mode decomposition. Therefore, the noise variance of the three groups of images is selected as 0.05, and the effective IMF components are selected by comparing the evaluation indexes of the modal components after decomposition. In the two-dimensional variational mode decomposition, the penalty parameter is  $\alpha = 5000$  and the mode number is  $k = 4$ . Fig.2, Fig.3 and Fig.4 respectively show the decomposed model components of the ultrasound kidney image, ultrasound fetal image, and standard image.

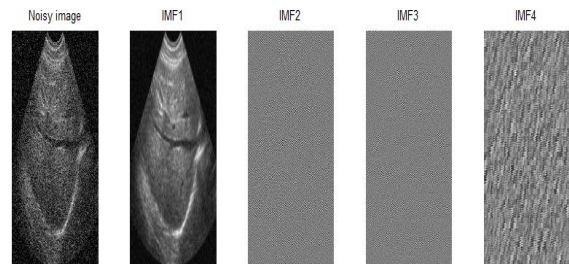


Figure 2. Decomposition picture of ultrasound kidney

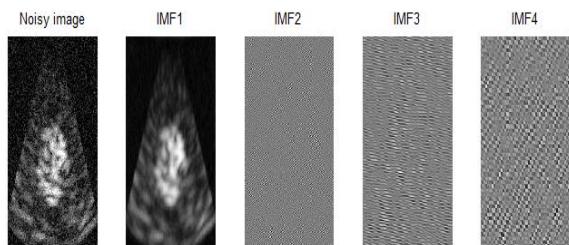


Figure 3. Decomposition picture of ultrasound fetus

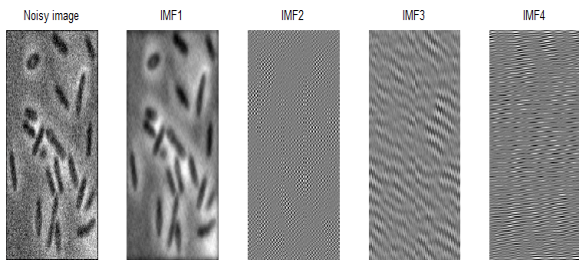


Figure 4. Decomposition picture of standard image

Fig.2, Fig.3and Fig.4 respectively show that three groups of images are decomposed to obtain four different modal components, and each component represents the information characteristics of different frequency bands in the original image.From the three groups of image decomposition diagrams,the first model component IMF1 can well retain the information in the original image and has less noise components,the IMF2 component has partial contour details of the original image but more noise components,IMF3 and IMF4 contain almost no information features of the original image and the noise component is quite large.In order to filter out the effective components, the peak signal-to-noise ratio and the root mean square error of the model components in the three groups of images are compared, as in Table.1.

Table.1 Comparison of IMF component indexes

Image	index	IMF1	IMF2	IMF3	IMF4
Ultrasound kidney	PSNR	28.413	10.666	10.666	10.572
	RMSE	10.714	62.669	61.510	62.740
Ultrasound fetus	PSNR	25.483	11.971	12.023	11.516
	RMSE	18.165	66.126	64.110	68.130
Standard image	PSNR	23.041	6.1540	5.8820	5.9676
	RMSE	21.656	116.59	118.88	117.72

According to the data in Table 1, the peak signal-to-noise ratio and root mean square error of the modal components in the three groups of ultrasound kidney, standard image, and ultrasound fetal images are relatively different.In terms of peak signal-to-noise ratio (PSNR), the difference between the first modal component IMF1 and other modal components is about 10 to 20,in addition,the difference between the first modal component IMF1 and other modal components is about 50 ~ 70 in root mean square error (RMSE).More importantly, the peak signal-to-noise ratio of the first modal component IMF1 is the highest and the root mean square error is the smallest,in addition,the peak signal-to-noise of other modal components IMF2, IMF3, and IMF4 is relatively low, the root mean square error is relatively high, and the difference in values between them is small.Therefore, the decomposed first modal components of the three groups of images can better

retain the information characteristics of the original image and have less noise components, so the first model component is determined as an effective component.The noise components of other model components IMF2, IMF3, and IMF4 are higher, which leads to the loss of the information characteristics of the original image, and then the other modal components are determined as noise components.By comparing the modal components of the three groups of ultrasound kidney, standard image and ultrasound fetal image,the first component IMF1 of the three groups of images is used as an effective modal component but its modal component still contains less noise components.Thus, anisotropic diffusion filtering is performed on its effective components,finally,reconstructing the filtered effective component is the denoised image.

In the case of noise with different variances (0.02、0.05),the effective modal components of the three groups of images decomposed by 2D-VDM are filtered by five methods.The two indicators of peak signal-to-noise ratio and root mean square error are used to measure the denoising performance of the five methods. The comparison of the PSNR values of the five methods is as in Table.2.

Table.2 PSNR Compare

Image	PSNR					
	variance	Wien er filter	Median Filter	2D-VDM +Median Filter	PM Filter	article method
Ultrasound kidney	0.02	26.85	27.89	28.96	22.49	28.53
	0.05	23.45	23.82	27.44	22.46	28.83
Ultrasound fetus	0.02	28.15	28.29	27.48	23.80	28.72
	0.05	24.77	24.31	26.30	22.56	27.99
Standard image	0.02	25.61	25.40	27.64	24.75	28.70
	0.05	24.52	24.64	26.82	25.00	27.99

According to the data in Table 2,Compared with other methods, this method has the highest peak signal-to-noise ratio and is about 1 ~ 0.2 higher than other methods, indicating that this method is superior to other methods in removing noise.From different noise densities, as the noise density increases, the method in this paper has less volatility in peak signal-to-noise ratio than other methods. In other words, the noise removal performance of other methods is greatly affected by the image noise density.In order to

measure the performance of each method in protecting details, the RMSE values of the five methods are as in Table 3.

**Table.3 RMSE Compare**

Image	variance	RMSE				
		Wiener filter	Median filter	2D-VD M+ Median Filter	PM Filter	Article method
Ultrasound kidney	0.02	13.46	12.02	10.90	14.11	10.56
	0.05	17.96	17.01	16.90	17.54	16.01
Ultrasound fetus	0.02	13.936	12.6182	12.9081	13.2700	12.5247
	0.05	18.405	18.425	18.3858	18.8538	18.1048
Standard image	0.02	16.956	16.598	13.1058	15.6441	12.0709
	0.05	17.738	15.5005	14.8314	15.3772	13.539

According to the data in Table 3, In terms of root mean square error (RMSE), compared with other methods, this method has the smallest root-mean-square error and the difference between other methods is about 1.1 ~ 0.2, which shows that this method is superior to other methods in protecting detailed information. According to the analysis of Table 2 and Table 3, in the case of different variance noise, the method in this paper is superior to other methods in terms of peak signal-to-noise ratio and root mean square error, indicating that the method in this paper can improve the denoising effect while retaining detailed information.

In order to better compare the visual effects of each method, Fig.5、Fig.6 and Fig.7 respectively show the effect of each method on denoising the ultrasound kidney, ultrasound fetus and standard image under the noise variance of 0.02.

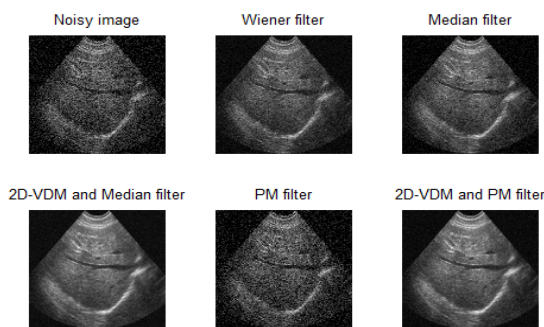


Figure 5. Comparison results of various methods

of ultrasound kidney

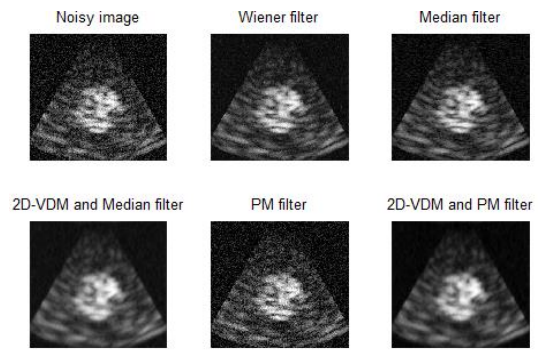


Figure 6. Comparison results of various methods

of ultrasound fetus

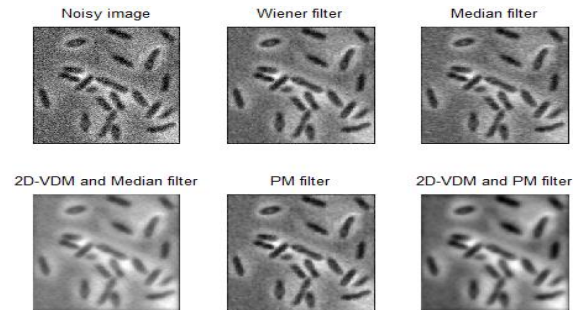


Figure 7. Comparison results of various methods

of standard charts

According to Fig. 5、Fig.6 and Fig.7, this paper applies a combination of two-dimensional variational mode decomposition and anisotropic diffusion to ultrasound images, and the results show that its denoising effect is better than other methods. Two-dimensional variational mode decomposition can decompose its image into low-frequency components and high-frequency components. In addition, for processing ultrasound images, anisotropic diffusion filtering is better than other filtering methods in terms of denoising effect and retaining detailed information. Therefore, this paper combines the characteristics of its two methods.

## 6. ACKNOWLEDGMENTS

For the problem of how to suppress the noise of the ultrasound image and protect its detailed information, this paper mainly applies the combination of two-dimensional variational mode decomposition and anisotropic diffusion to the ultrasound image. Two-dimensional variational mode decomposition can decompose its image into low-frequency components and high-frequency components. In addition, for processing ultrasound images, anisotropic diffusion filtering is better than other filtering methods in terms of denoising effect and retaining detailed information. Therefore, this paper combines the characteristics of its two methods. In addition, the peak signal-to-noise ratio and root mean square error are mainly selected as the performance indicators of the algorithm. From the experimental results, the algorithm in this paper is superior to other algorithms in removing noise in the ultrasound image and retaining the original details. The

method in this paper works well in removing noise, but there are some shortcomings, such as the slower decomposition speed of 2D modal decomposition and the selection of the appropriate number of modal decomposition.

## 7. REFERENCES

- [1] Lu Zhaoling. Development trend of medical ultrasound diagnosis [J]. *Applied Acoustics*, 2008, 27(4): 245–24
- [2] Christos P. Loizou, Constantinos S. Pattichis. *Despeckle Filtering Algorithms and Software for Ultrasound Imaging* [M]. Morgan & Claypool Publishers series, 2008: 45-74.
- [3] Wang Yaqiang, Chen Bo. An improved anisotropic diffusion ultrasonic image denoising algorithm [J]. *Liquid Crystal and Display*, 2015, 30(2): 30-36
- [4] He Peipei. Image Denoising Based on BEMD [J]. *Computer Simulation*, 2009, 26(1): 216-218.
- [5] Dragomiretskiy K, Zosso D. Variational Mode Decomposition [J]. *IEEE Transactions on Signal Processing*, 2014, 62(3): 531-544.
- [6] Dragomiretskiy K, Zosso D. Two-dimensional variational mode de-composition [J]. *Springer International Publishing*, 2015, 65(3): 197-208.
- [7] Li Xiang, Wang Wenbo. De-noising method of hyperspectral image based on two-dimensional empirical mode decomposition [J]. *Laser and Infrared*, 2013, 43(11): 1311-1315.
- [8] Leng Chengcai, Zhao Fengqun, Dai Fang. Improvement of P-M model diffusion function [J]. *Computer and Modernization*, 2008, 40(1): 19-20.
- [9] Wang Yaqiang, Chen Bo et al. An improved anisotropic diffusion ultrasonic image denoising algorithm [J]. *Liquid Crystal and Display*, 2015, 30(2): 30-36.
- [10] Pang Jianxin. Research on objective evaluation of image quality [D]. PhD thesis, University of Science and Technology of China, 2008.
- [11] M. Szczypinski, M. Strzelecki, A. Materka, A. Klepaczko, MaZda. A software package for image texture analysis, *Comp[J]. Methods Prog. Biomed*, 2008, 94(1): 66–76
- [12] Christos P. Loizou, Constantinos S. Pattichis. Comparative Evaluation of Despeckle Filtering In Ultrasound Imaging of the Carotid Artery [J]. *IEEE transactions on ultrasonics, ferroelectrics, and frequency control*, 2005, 52(10): 53- 64
- [13] Zhou Guirong, Li Delai. Design Simulation of Ultrasonic Beam Formation Using Field-II [J]. *China Medical Device Information Press*, 2015. 36(3): 31-38.
- [14] Shi Yazheng. Simulation and Realization of Ultrasound Image Processing [D]. Master Thesis of University of Electronic Science and Technology of China, 2010.
- [15] Liu Jiamin, Peng Ling, Yuan Jiacheng, Liu Junwei. Image denoising method based on two-dimensional variational mode decomposition and adaptive median filtering [J]. *Computer Application Research*, 2017. 36(10): 32-37.
- [16] Chang Qiuhan. Application of Variational Modal Decomposition in Medical Images [D]. Master Thesis of Northeast Petroleum University, 2018.